1

2

3 **Disabling Cas9 by an anti-CRISPR DNA mimic**

4

5 Jiyung Shin[1,2]*, Fuguo Jiang[2]*, Jun-Jie Liu[2,5]*, Nicolas L. Bray[1,2], Benjamin J. Rauch[3],

6 Seung Hyun Baik[1,2] , Eva Nogales[2,5], Joseph Bondy-Denomy[3], Jacob E. Corn[1,2]† and

7 Jennifer A. Doudna[1,2,4,5]†

8

9

10

11 [1]Innovative Genomics Institute, [2]Department of Molecular and Cell Biology, University of

12 California, Berkeley, California 94720; [3]Department of Microbiology and Immunology,

13 and Quantitative Biosciences Institute, University of California, San Francisco, CA

14 94158; [4]Howard Hughes Medical Institute; [5]Department of Chemistry, University of

15 California, Berkeley, California 94720; [5]Molecular Biophysics and Integrated Bioimaging

16 Division, Lawrence Berkeley National Laboratory, Berkeley, California 94720

17

18 *These authors contributed equally to the project.

19 †Correspondence should be addressed to J.E.C. (jcorn@berkeley.edu) and J.A.D.

20 (doudna@berkeley.edu)

21

22    **CRISPR-Cas9 gene editing technology is derived from a microbial adaptive**

23    **immune system, where bacteriophages are often the intended target. Natural**

24    **inhibitors of CRISPR-Cas9 enable phages to evade immunity and show promise**

25    **in controlling Cas9-mediated gene editing in human cells. However, the**

26    **mechanism of CRISPR-Cas9 inhibition is not known and the potential**

27    **applications for Cas9 inhibitor proteins in mammalian cells has not fully been**

28    **established. We show here that the anti-CRISPR protein AcrIIA4 binds only to**

29    **assembled Cas9-single guide RNA (sgRNA) complexes and not to Cas9 protein**

30    **alone. A 3.9 Å resolution cryo-EM structure of the Cas9-sgRNA-AcrIIA4 complex**

31    **revealed that the surface of AcrIIA4 is highly acidic and binds with 1:1**

32    **stoichiometry to a region of Cas9 that normally engages the DNA protospacer**

33    **adjacent motif (PAM). Consistent with this binding mode, order-of-addition**

34    **experiments showed that AcrIIA4 interferes with DNA recognition but has no**

35    **effect on pre-formed Cas9-sgRNA-DNA complexes. Timed delivery of AcrIIA4 into**

36    **human cells as either protein or expression plasmid allows on-target Cas9-**

37    **mediated gene editing while reducing off-target edits.  These results provide a**

38    **mechanistic understanding of AcrIIA4 function and demonstrate that inhibitors**

39    **can modulate the extent and outcomes of Cas9-mediated gene editing.**

40

41

2

42    Phage-encoded inhibitors of CRISPR-Cas bacterial immune systems evolved to enable

43    phage escape from destruction in bacterial cells (*1*) and have the potential to control

44    CRISPR-Cas enzymes that are deployed for gene editing applications in various cell

45    types (*2, 3*). Determination of the molecular basis for Cas9 inhibition could shed light on

46    the evolutionary "arms race" between phage and bacteria, as well as suggest new

47    approaches to regulate genome editing in eukaryotic cells.  The 87 amino acid anti-

48    CRISPR-Cas9 protein AcrIIA4 is notable in both respects: it inhibits multiple Cas9

49    proteins including the widely used Cas9 ortholog from *Streptococcus pyogenes* (Spy),

50    and it blocks Cas9-mediated gene editing in human cells (*3*). To investigate the

51    molecular basis for AcrIIA4-mediated Cas9 inhibition, we first tested whether

52    recombinant AcrIIA4 protein interacts directly with SpyCas9 (Fig. 1A). Purified AcrIIA4

53    was incubated with *Spy*Cas9 in the presence or absence of a single-guide RNA

54    (sgRNA) that assembles with Cas9 to provide sequence-specific DNA recognition (*4*).

55    Size exclusion chromatography showed that AcrIIA4 binds to SpyCas9 only in the

56    presence of sgRNA (Fig. 1B and C, fig. S1), implying that AcrIIA4 recognizes a protein

57    surface created upon sgRNA-triggered conformational rearrangement (*5, 6*).

58    Furthermore, the AcrIIA4-bound Cas9-sgRNA complex is more resistant to proteolytic

59    digestion than the Cas9-sgRNA complex alone, implying that AcrIIA4 stabilizes a

60    particular Cas9 conformation (fig. S2).

61         To elucidate the molecular basis of AcrIIA4-mediated inhibition of Cas9 activity,

62    we performed cryo-electron microscopy (cryo-EM) single-particle analysis on a

63    SpyCas9-sgRNA complex bound to AcrIIA4. Cryo-EM images were collected on a Krios

3

64 microscope using zero-loss energy-filtered imaging and a K2 direct electron detector.

65 After unsupervised 3D classification of 840,000 particle images, refinement of a class

66 containing 285,600 particles resulted in an EM reconstruction of the SpyCas9-sgRNA-

67 AcrIIA4 complex with an overall resolution of 3.9 Å (fig. S3-S4). Subsequent local 3D

68 classification that was focused on Cas9's HNH nuclease domain ultimately yielded two

69 EM reconstructions, one at 3.9 Å resolution where the HNH was poorly resolved due to

70 flexibility (reconstruction 1, obtained as a combination of two 3D classes) (Fig. 2a and

71 fig. S5a) and one with better defined density for the HNH domain at an average

72 resolution of 4.5 Å (reconstruction 2) (fig. S4d and S5a; see Methods section and fig.

73 S3). In both cryo-EM reconstructions, the density for the HNH domain of Cas9 was

74 weaker than for the rest of the structure, consistent with the previously observed

75 conformational plasticity of the HNH nuclease domain in the pre-targeting state. An

76 atomic model for AcrIIA4 was built from reconstruction 1. The EM density map displays

77 excellent main-chain connectivity and side-chain densities for almost all residues of

78 AcrIIA4 (fig. S5). We then built an atomic model for the Cas9-sgRNA complex based on

79 the crystal structure of SpyCas9-sgRNA (PDB ID 4ZT0) and refined the entire SpyCas9-

80 sgRNA-AcrIIA4 model in real space to good stereochemistry (Fig. 2B and table S1).

81 Overall, Cas9 bound to AcrIIA4 resembles the pre-target state rather than the DNA-

82 bound state (fig. S6).

83  *De novo* model building demonstrated that AcrIIA4 binds to Cas9 with 1:1

84 stoichiometry and comprises a three-stranded antiparallel β sheet flanked by one alpha-

85 helix at the amino-terminal end and two α helices on the carboxy-terminal end

4

86 ($\alpha_1\beta_1\beta_2\beta_3\alpha_2\alpha_3$). Remarkably, superposition of the AcrIIA4-bound Cas9 structure with

87 DNA-bound Cas9 revealed that AcrIIA4 sits exactly in the PAM-interacting cleft formed

88 between the alpha-helical recognition (REC) lobe and the nuclease lobe (Fig. 2B and

89 fig. S6). AcrIIA4 completely occupies the PAM binding pocket and thus blocks DNA

90 recognition through contacts between the $\beta3$ strand of AcrIIA4 and Cas9 PAM-binding

91 residues (R1333 and R1335) (Fig. 2D-E). In addition, AcrIIA4 wedges into the DNA

92 melting region immediately upstream of the PAM sequence and sits on top of +1

93 phosphate on the target strand and the flipped nucleotides on the nontarget strand,

94 indicating AcrIIA4 could also prevent DNA binding/unwinding. Consistent with this DNA-

95 mimicing binding mode, AcrIIA4 is extremely acidic (Fig. 2E). Interestingly, AcrIIA4 also

96 occupies the same space as the DNA-bound HNH domain and the linker connecting the

97 HNH and RuvC domains (Fig. 2D), suggesting AcrIIA4 could block the HNH movement

98 required for catalysis (Fig. 2B, C).

99       Collectively, our structural studies show that AcrIIA4 is a highly acidic DNA mimic

100 that blocks target DNA recognition through multiple mechanisms: 1) competitive

101 inhibition of PAM binding; 2) inhibition of DNA unwinding upstream of the PAM

102 sequence; and 3) inactivation of HNH domain movement from the inactive to active

103 conformation. These structural findings help explain the effectiveness of AcrIIA4 as an

104 inhibitor of Cas9-mediated DNA cleavage and cell-based genome editing. Previous

105 studies revealed the importance of Cas9's interactions with targeted DNA, mediated via

106 the PAM in an interaction preceding base pairing between the sgRNA and its target (7).

107 Transient Cas9-sgRNA association with PAM sequences in DNA is thought to enable a

5

108     rapid target sequence search. By mimicking the structure and electrostatic properties of

109     the DNA PAM sequence, AcrIIA4 might compete for initial DNA binding and thereby

110     prevent target recognition and cleavage (Fig. 2E-G).

111         To determine the functional effects of AcrIIA4 binding to Cas9-sgRNA

112     complexes, we subjected DNA substrates possessing a target sequence to Cas9-

113     sgRNA-catalyzed DNA cleavage assays. A linearized plasmid possessing a target

114     sequence and PAM was incubated with combinations of Cas9, sgRNA and AcrIIA4, and

115     the products were resolved by gel electrophoresis. Cas9-sgRNA alone completely cut

116     the target DNA within five minutes, while AcrIIA4 limited cleavage at even later time

117     points (Fig. 3A). To confirm that AcrIIA4 would also inactivate Cas9 at low enzyme and

118     inhibitor concentrations, we performed similar experiments with a radiolabeled DNA

119     target for increased sensitivity (Fig. 3B). Near-stoichiometric concentrations of AcrIIA4

120     inhibited DNA cleavage when titrated against 10 nM Cas9-gRNA complex, indicating an

121     apparent dissociation constant of less than 10 nM. These data show that AcrIIA4

122     functions as a robust Cas9 "off-switch" that can inhibit most Cas9 activity at low

123     concentrations.

124         The structure of Cas9 bound to AcrIIA4 suggested that the inhibitor competes for

125     the initial DNA recognition event of PAM binding. Yet we previously found that Cas9

126     binds so tightly to target DNA that its off-rate is negligible (*7, 8*). This implies an unusual

127     non-equilibrium mode of inhibition, in which AcrIIA4 requires access to Cas9-sgRNA

128     prior to formation of the Cas9-sgRNA-DNA complex. To test this prediction, we used

129     bilayer interferometry to measure the binding of catalytically inactivated Cas9 (dCas9) to

130   a DNA target in the presence of inhibitor. These experiments were performed under

131   stoichiometric binding conditions in which Cas9 was present at concentrations greater

132   than the dissociation constant of the Cas9-AcrIIA4 interaction. Pre-incubation of Cas9

133   with AcrIIA4 markedly inhibited Cas9 binding to DNA (on-rate) in a dose-dependent

134   fashion, including complete prevention of target engagement (Fig. 3C, fig. S7). An

135   electrophoretic mobility shift assay (EMSA) further confirmed that AcrIIA4 does not

136   impact sgRNA loading into Cas9 protein alone (fig. S8), but does inhibit Cas9-sgRNA

137   complex binding to a target DNA (fig. S9). Strikingly, allowing the Cas9-sgRNA-DNA

138   complex to form and then adding AcrIIA4 had no effect on Cas9's release of target DNA

139   (off-rate). These order-of-addition results are consistent with both the structure of

140   AcrIIA4 bound to Cas9 and Cas9's extremely slow dissociation from DNA. Together,

141   these data support a mechanism for AcrIIA4 inhibition in which the inhibitor blocks

142   Cas9's ability to bind and cut target DNA by obscuring the PAM-interacting domain.

143       To determine the ability of AcrIIA4 to regulate gene editing in human cells, we

144   first utilized human K562 erythroleukemia cells stably expressing a chromosomally-

145   integrated blue fluorescent protein (BFP) reporter (8). Nucleofection of Cas9-sgRNA

146   (Cas9 RNP) complexes targeting BFP resulted in loss of BFP fluorescence in almost all

147   cells as measured by flow cytometry (fig. S10). Simultaneous delivery of Cas9 RNP and

148   AcrIIA4 protein inhibited Cas9-mediated gene targeting by up to 80% (Fig. 4A blue

149   symbols; fig. S10). Simultaneous delivery of AcrIIA4 encoded in a plasmid inhibited

150   gene editing to a lesser extent, possibly due to a delay in expression of the inhibitor

151   from a plasmid relative to immediate nucleofection of Cas9 RNP (Fig. 4A green

7

152     symbols; fig. S10, S11). This implied that the order-of-addition effects we observed in

153     biophysical experiments may play a role during gene editing. To test this idea, we

154     nucleofected AcrIIA4 plasmid 24 hours prior to introducing Cas9 RNP into cells. The

155     presence of the AcrIIA4-encoding plasmid 24 hours prior to Cas9 RNP introduction

156     inhibited Cas9-mediated gene targeting to a far greater extent than was observed

157     during co-introduction, and to a similar extent as observed during co-introduction of

158     AcrIIA4 protein and Cas9 RNP (Fig. 4B, fig. S12). Remarkably, we found that addition of

159     AcrIIA4 six hours after Cas9-RNP reduced editing by ~50%, demonstrating the utility of

160     inhibitors for revealing *in vivo* gene editing kinetics (Fig. 4C, fig. S13). In sum,

161     controlling the timing of AcrIIA4 inhibition in human cells strongly affects the frequency

162     of gene editing at a given locus.

163         Using a given guide RNA, Cas9 may target both an on-target site and off-target

164     loci (*9-12*). But several lines of evidence suggest that off-target sites may be bound

165     without being immediately cleaved (*13-15*). Cas9 displaced from uncleaved sites (e.g.

166     by cellular factors) would be available for inhibition by AcrIIA4. Since inhibitor timing

167     experiments suggested that at least 50% of on-target Cas9 gene editing takes place

168     within the first 6 hours (Fig. 4C), we asked whether off-target editing could be reduced

169     by properly timed addition of inhibitor.

170         We examined on- and off-target editing using guide RNAs targeting the EMX1

171     and HBB loci. The off-target sites for both the EMX1 and HBB guides have been

172     previously described (*10, 16, 17*). Notably, the HBB guide is of therapeutic interest to

173     edit the causative mutation of sickle cell disease, but has an off-target that is nearly

8

174    identical to the on-target site. We edited the EMX1 and HBB loci using Cas9 RNPs with

175    and without pre-introduction of AcrIIA4 protein or plasmid. Consistent with experiments

176    at the BFP locus, we found that timed addition of AcrIIA4 retained substantial levels of

177    on-target editing. Strikingly, both T7E1 and TIDE analysis showed that timed addition of

178    AcrIIA4 almost completely abolished off-target editing at both HBB and EMX1 (Fig. 4D).

179    This suggests that Cas9 inhibitors have the potential to be useful in reducing off-target

180    events during research and therapeutic applications.

181        The recent and rapid expansion of the Cas9 toolkit for gene editing applications

182    has lacked an inducible "off-switch" to prevent undesired gene editing. Newly

183    discovered protein inhibitors, encoded by bacteriophages, provide an attractive solution

184    to this problem as these proteins are small and function well in human cells (*3*). Here,

185    we demonstrate that AcrIIA4, the most potent SpyCas9 inhibitor in human cells, acts as

186    a DNA mimic to block PAM recognition. The deployment of DNA mimics to inhibit a

187    DNA-binding protein is an elegant solution that is often deployed in the phage-host arms

188    race. A recent structural study revealed that a Class 1 anti-CRISPR (AcrF2) uses a

189    similar strategy (*18*). Further, phage-encoded restriction enzyme inhibitor proteins have

190    long been known to mimic the DNA target (*19*). Our results further show that Cas9

191    inhibitors delivered as either protein or expressed from a plasmid can modulate the

192    efficacy of gene editing at multiple loci in human cells. Although pre-addition of inhibitor

193    almost completely abolishes overall gene editing, timed addition of inhibitor after

194    initiating Cas9-sgRNA-based gene editing can adjust the amount of time that Cas9 is

195    active in the nucleus, thereby selectively limiting off-target editing. We anticipate that

9

196    Cas9 inhibitors could be broadly useful in situations where precise control of either on-

197    or off-target gene editing is desirable, such as during allele-specific therapeutic editing.

198

199

200    **Figures**



201
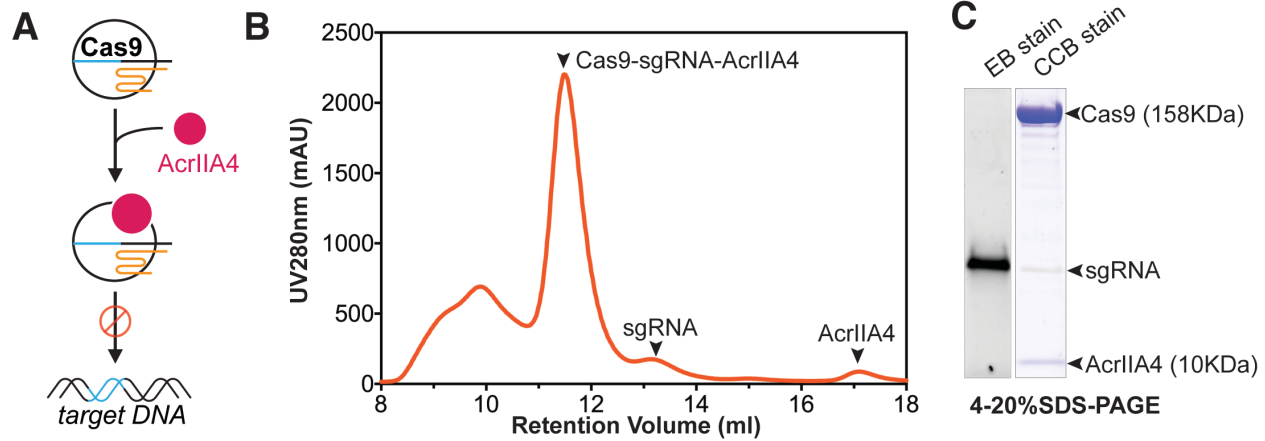
**Fig 1. AcrIIA4 binds to the *S. pyogenes* Cas9-sgRNA complex.**

203    A) A cartoon depiction of Cas9 protein loaded with the sgRNA binding to AcrIIA4

204        (pink). Cas9-sgRNA complexed with AcrIIA4 is unable to bind to the target DNA.

205    B) Size exclusion chromatogram of SpyCas9-sgRNA after preincubation with

206        AcrIIA4. Relevant peaks are indicated with arrowheads.

207    C) Coomassie and Ethidium Bromide (EB) stained polyacrylamide gel showing the

208        commigration of AcrIIA4 with Cas9 in the presence of guide RNA.

209

210
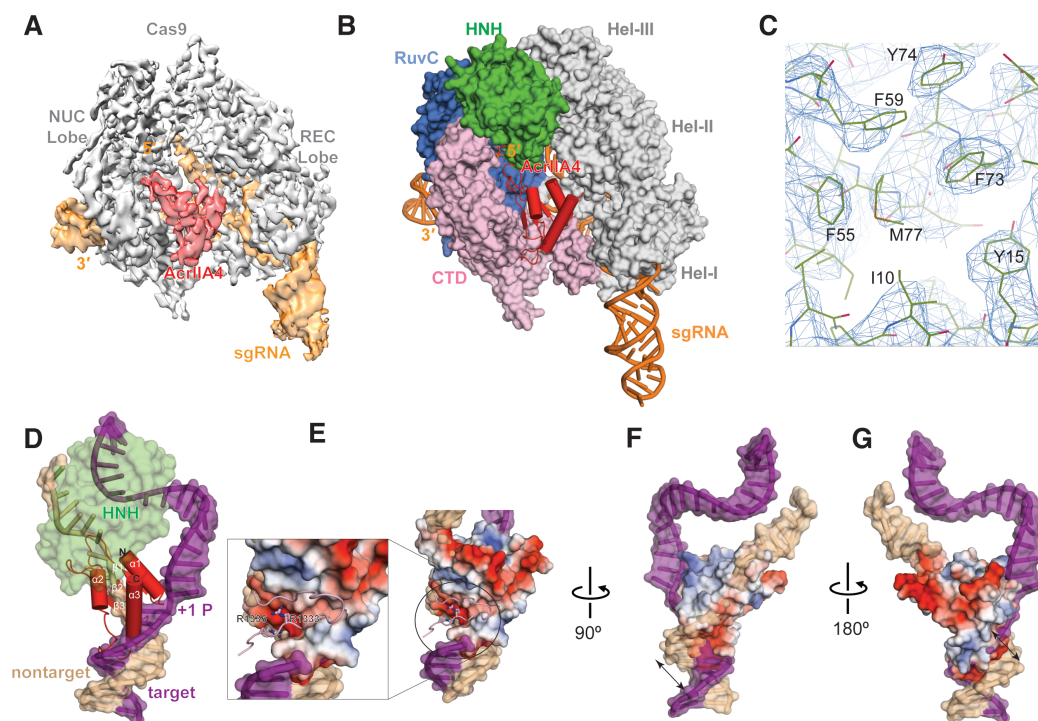
**Fig. 2. Architecture of the *S. pyogenes* Cas9-sgRNA in complex with AcrIIA4**

A) Cryo-EM reconstruction of the AcrII4-bound SpyCas9. The electron density map was contoured at high threshold levels showing distinct features for each subunit.

B) The atomic model of SpyCas9-sgRNA-ArcrIIA4. AcrIIA4 (red) and sgRNA (orange) are shown in ribbon diagram and SpyCas9 is displayed as surface representation.

C) Representative region (hydrophobic core) of the cryo-EM density for AcrIIA4 with the refined model superimposed.

D) Superposition with Cas9-guideRNA-dsDNA structure (PDB ID 5F9R). For clarity, Cas9 is omitted except the HNH domain. Target and nontarget DNA strand is is

12

221     colored purple and beige, respectively.

222   E)  Electrostatic surface potential of AcrIIA4. The inset shows the PAM recognition

223       residues (R1333 and R1334) are largely buried in an acidic pocket within

224       AcrIIA4.

225   F)  and G) Close-up of AcrIIA4 binding pocket at different views showing AcrIIA4 is a

226       dsDNA mimic.

227

13

228
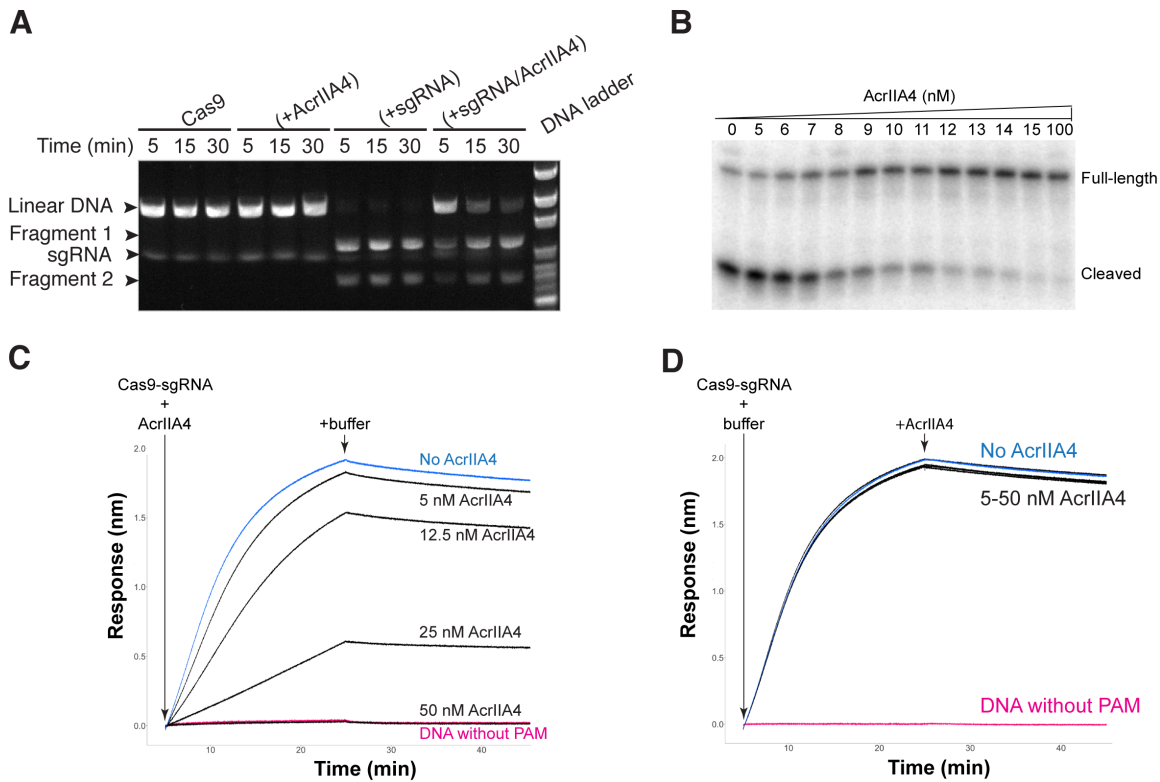
**Fig. 3. AcrIIA4 inhibits DNA cleavage *in vitro***

A) A linearized plasmid was incubated with Cas9 alone, AcrIIA4 alone, Cas9 + sgRNA, or Cas9 + sgRNA + AcrIIA4 for 5, 15, or 30 minutes. Reactions were resolved via agarose gel electrophoresis and visualized by ethidium bromide staining.

B) AcrIIA4 inhibits SpyCas9 cleavage of radiolabeled target DNA *in vitro*. 10 nM SpyCas9-crRNA-tracrRNA complex were pre-incubated with increasing concentrations (0-100 nM) of AcrIIA4. Sub-stoichiometric synthetic oligonucleotide duplexes (2.5 nM) bearing a radiolabel at the 5' end of the complementary strand, were introduced for 6-minute cleavage reactions. Reactions were resolved by denaturing polyacrylamide gel electrophoresis and visualized by

14

240    phosphorimaging.

241  C) AcrIIA4 inhibits dCas9-sgRNA binding to a DNA target but does not affect target

242    release, as measured by biolayer interferometry. Pre-incubating increasing

243    concentrations of AcrIIA4 with dCas9-sgRNA reduces the on-rate of association

244    with a DNA target relative to no inhibitor (blue). Maximal inhibition is identical to

245    dCas9-sgRNA added to target DNA with a PAM mutation (red).

246  D) Addition of increasing concentrations of AcrIIA4 with pre-formed dCas9-sgRNA-

247    DNA complex has no effect upon the off-rate of dissociation.

248
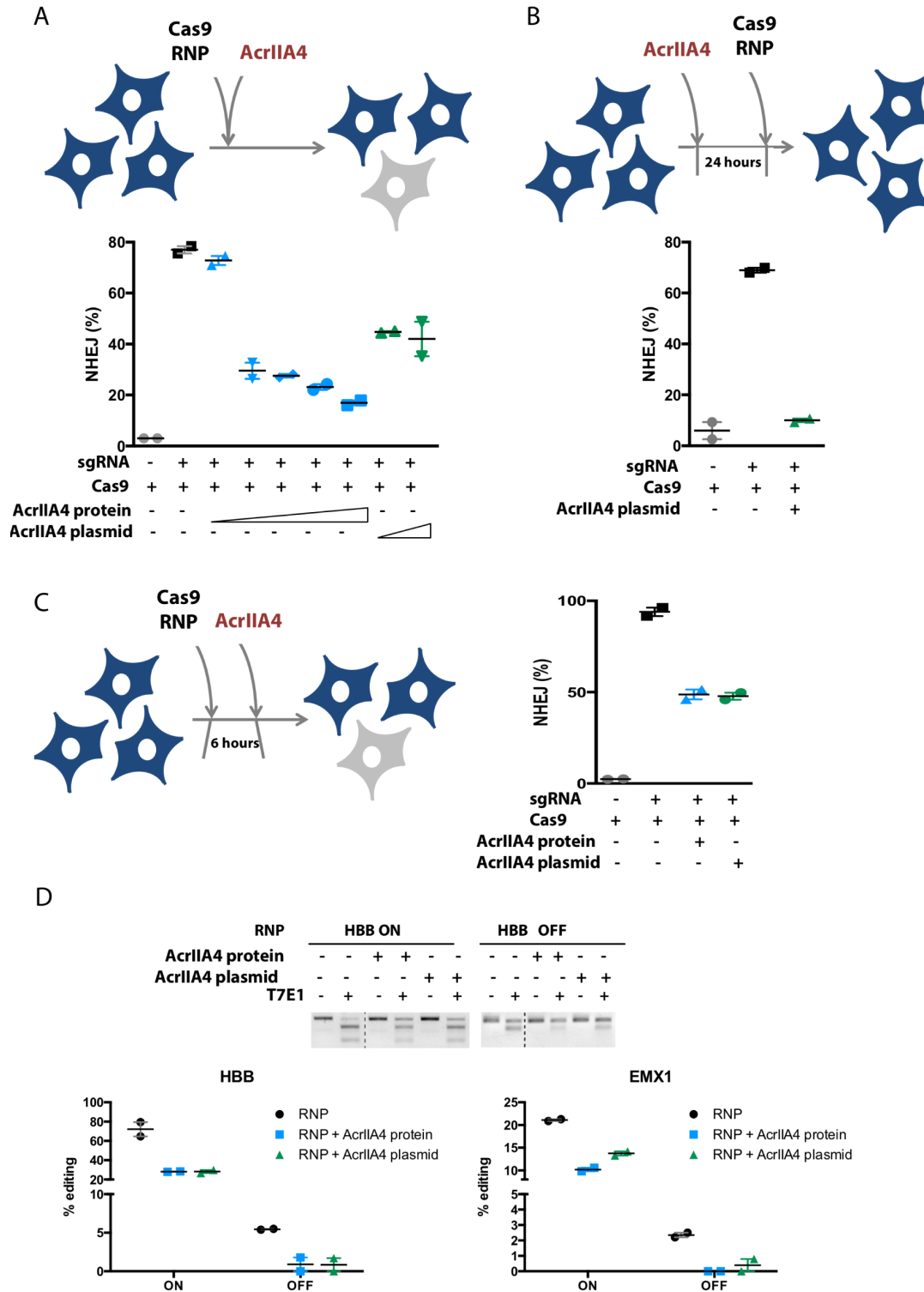
**Fig. 4. Timed delivery of AcrIIA4 differentially inhibits on- and off-target genome**

251 **editing in human cells.**

252     A)  Simultaneous delivery of Cas9 RNP and AcrIIA4 inhibits Cas9-mediated gene

253         targeting in human cells. K562 cells with a chromosomally integrated BFP (BFP-

254         K562) were nucleofected with Cas9 RNP and AcrIIA4 protein (Cas9:AcrIIA4

255         (molar ratio), 1:0.5, 1:1, 1:2, 1:3, 1:5) or plasmid (0.7µg and 2.8µg). NHEJ

256         frequencies are quantified by loss of BFP expression in BFP-K562 cells 96 hours

257         post nucleofection via flow cytometry. Data presented as mean ± SEM from at

258         least two biological replicates.

259     B)  Administration of AcrIIA4 prior to Cas9 RNP completely inhibits Cas9-mediated

260         gene targeting.  BFP-K562 cells were nucleofected with AcrIIA4 plasmid (0.7µg)

261         24 hours prior to Cas9 RNP delivery. Data presented as mean ± SEM from at

262         least two biological replicates.

263     C)  Delivery of AcrIIA4 after introduction of Cas9 RNP yields intermediate inhibition

264         of Cas9 activity. BFP-K562 cells were nucleofected with AcrIIA4 protein

265         (Cas9:AcrIIA4 (molar ratio), 1:5) or plasmid (0.7µg) 6 hours post Cas9 RNP

266         delivery. Data presented as mean ± SEM from at least two biological replicates.

267     D)  Proper timing of AcrIIA4 delivery diminishes off-target editing events while largely

268         retaining on-target editing. K562 cells were nucleofected with either HBB or

269         EMX1 targeting Cas9 RNP 6 hours prior to AcrIIA4 protein (Cas9:AcrIIA4 (molar

270         ratio), 1:5) or plasmid (0.7µg) delivery. (Top) Representative T7 endonuclease I

271         assay for visualization of HBB on- and off- target editing. (Bottom) Quantification

272         of on- and off-target editing at HBB and EMX1, as measured by TIDE analysis.

17

273 **References**

274 1.    J. Bondy-Denomy, A. Pawluk, K. L. Maxwell, A. R. Davidson, Bacteriophage genes that

275          inactivate the CRISPR/Cas bacterial immune system. *Nature* **493**, 429-432 (2013).

276 2.    A. Pawluk *et al.*, Naturally Occurring Off-Switches for CRISPR-Cas9. *Cell* **167**, 1829-

277          1838 e1829 (2016).

278 3.    B. J. Rauch *et al.*, Inhibition of CRISPR-Cas9 with Bacteriophage Proteins. *Cell* **168**,

279          150-158 e110 (2017).

280 4.    M. Jinek *et al.*, A programmable dual-RNA-guided DNA endonuclease in adaptive

281          bacterial immunity. *Science* **337**, 816-821 (2012).

282 5.    M. Jinek *et al.*, Structures of Cas9 endonucleases reveal RNA-mediated

283          conformational activation. *Science* **343**, 1247997 (2014).

284 6.    H. Nishimasu *et al.*, Crystal structure of Cas9 in complex with guide RNA and target

285          DNA. *Cell* **156**, 935-949 (2014).

286 7.    S. H. Sternberg, S. Redding, M. Jinek, E. C. Greene, J. A. Doudna, DNA interrogation by

287          the CRISPR RNA-guided endonuclease Cas9. *Nature* **507**, 62-67 (2014).

288 8.    C. D. Richardson, G. J. Ray, M. A. DeWitt, G. L. Curie, J. E. Corn, Enhancing homology-

289          directed genome editing by catalytically active and inactive CRISPR-Cas9 using

290          asymmetric donor DNA. *Nat Biotechnol* **34**, 339-344 (2016).

291 9.    Y. Fu *et al.*, High-frequency off-target mutagenesis induced by CRISPR-Cas nucleases

292          in human cells. *Nat Biotechnol* **31**, 822-826 (2013).

293 10.   P. D. Hsu *et al.*, DNA targeting specificity of RNA-guided Cas9 nucleases. *Nat

294          Biotechnol* **31**, 827-832 (2013).

295  11.  P. Mali *et al.*, CAS9 transcriptional activators for target specificity screening and

296       paired nickases for cooperative genome engineering. *Nat Biotechnol* **31**, 833-838

297       (2013).

298  12.  V. Pattanayak *et al.*, High-throughput profiling of off-target DNA cleavage reveals

299       RNA-programmed Cas9 nuclease specificity. *Nat Biotechnol* **31**, 839-843 (2013).

300  13.  S. Kiani *et al.*, Cas9 gRNA engineering for genome editing, activation and repression.

301       *Nat Methods* **12**, 1051-1054 (2015).

302  14.  S. H. Sternberg, B. LaFrance, M. Kaplan, J. A. Doudna, Conformational control of DNA

303       target cleavage by CRISPR-Cas9. *Nature* **527**, 110-113 (2015).

304  15.  X. Wu *et al.*, Genome-wide binding of the CRISPR endonuclease Cas9 in mammalian

305       cells. *Nat Biotechnol* **32**, 670-676 (2014).

306  16.  T. J. Cradick, E. J. Fine, C. J. Antico, G. Bao, CRISPR/Cas9 systems targeting beta-

307       globin and CCR5 genes have substantial off-target activity. *Nucleic Acids Res* **41**,

308       9584-9592 (2013).

309  17.  M. A. DeWitt *et al.*, Selection-free genome editing of the sickle mutation in human

310       adult hematopoietic stem/progenitor cells. *Sci Transl Med* **8**, 360ra134 (2016).

311  18.  S. Chowdhury *et al.*, Structure Reveals Mechanisms of Viral Suppressors that

312       Intercept a CRISPR RNA-Guided Surveillance Complex. *Cell* **169**, 47-57 e11 (2017).

313  19.  M. D. Walkinshaw *et al.*, Structure of Ocr from bacteriophage T7, a protein that

314       mimics B-form DNA. *Mol Cell* **9**, 187-194 (2002).

315

316  **Acknowledgments**